Proceedings of the 2009 IEEE International Conference on Systems, Man, and Cybernetics
San Antonio, TX, USA - October 2009

# Spatial Correlation Analysis Using Canonical Correlation Decomposition for Sparse Sonar Array Processing

Yinghui Zhao, Mahmood R. Azimi-Sadjadi, Neil Wachowski, and Nick Klausner
Department of Electrical & Computer Engineering, Colorado State University
Fort Collins, CO 80523, USA
Email: azimi@engr.colostate.edu

***Abstract*—This paper uses the canonical correlation decomposition (CCD) framework to investigate the spatial correlation of sources captured using two spatially separated sensor arrays. The relationship between the canonical correlations of the observed signals and the spatial correlation coefficients of the source signals are first derived, including an analysis of the changes seen in this relationship under certain noise level and array geometry assumptions. Additionally, simulation results are presented that demonstrate the effects of different noise levels and array geometries on the canonical correlations for the case of two uniform linear sparse arrays.**

***Index Terms*—Canonical correlation decomposition, spatial correlation coefficient, covariance matrix**

## I. Introduction

As a method for determining the linear relationships between two sets of multi-dimensional random variables, Canonical Correlation Decomposition (CCD) [1] plays an important role in signal processing. The purpose in array signal processing is to extract the useful information such as directions of arrival (DOA) of the sources and their numbers from the received signals [2]. In many sonar applications, certain information about the sources, such as their locations, spectral properties, and statistical characteristics, is often desired. Since CCD performs multivariate statistical analysis and reveals the underlying coherence of the observed signals, it can be employed to extract this type of information based on a spatially separated array configuration.

CCD has been exploited in many studies [3]-[6] involving spatially separated array applications. In [3], CCD was used to determine the number of sources in an unknown noise environment for a bi-array system. In another study [4], various methods for determining the DOA of multiple source signals including MUSIC (MUltiple SIgnal Classification), UN-MUSIC (Unknown Noise-MUSIC), MLE (Maximum Likelihood Estimation), and UN-CLE (Unknown Noise-Correlation, and Location Estimation) were extended using a generalized correlation decomposition framework. These methods were subsequently used to estimate the DOA of sources in unknown correlated noise. The study in [5] demonstrated that using CCD with these methods resulted in optimum performance. In [6], it was proposed that CCD can be used to estimate the time-delay of the signals between two arrays, which can then be used to obtain a higher DOA estimation precision.

Apart from array processing applications, many implicit connections between canonical coordinate systems and two-channel signal systems have been explored. In [7], it is shown that the canonical correlations between a message signal and a measurement signal can be used to determine information rate and capacity. In another study that focused on two-channel constrained least squares (CLS) problems [8], canonical coordinate mapping matrices were derived by posing the problem as a coupled generalized eigenvalue problem. This eigenvalue problem establishes a connection between two-channel CLS filtering and transform methods for resolving channel measurements into canonical or half-canonical coordinates.

For sparse sonar array processing that is the focus of this study, each of the separated subarrays receives the signals from the same sources in the field. However, due to the motion of the sonar platform and signal fading effects in medium, the received signals at two spatially separated arrays will be different even for the same source. In [9], canonical correlation analysis was used to measure the signal coherence between pairs of sparse sensor arrays. CCD provides a powerful tool for analyzing the coherence between pairs of sparse sensor arrays. In this work, the spatial correlation of the sources are analyzed using the CCD of the collected data, and the connections between canonical correlations and source correlations are derived. This demonstrates that canonical correlations can be used to analyze the spatial correlations of the source signals. In particular, it is shown that the canonical correlations are equal to the spatial correlation coefficients for independent source signals when noise is not considered.

This paper is organized as follows. Section II describes the array signal model that is used in the subsequent derivations. Section III presents an analysis of the spatial correlation of the sources described by the given model using CCD. In Section IV, a special case where the signal correlations are only dependent on the sensor element spacing is investigated. The developments in this paper are then verified via simulation results provided in Section V, which includes results on the effects of different noise levels and the geometry between the sources and sonar arrays on the canonical correlations



978-1-4244-2794-9/09/$25.00 ©2009 IEEE

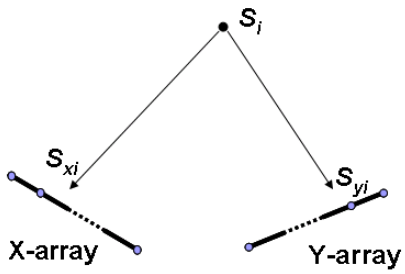


Fig. 1. Sparse Array Geometry.

produced by CCD. Finally, in Section VI, conclusions are drawn.

## II. Array Signal Model

Consider two uniform linear arrays, each of which has $M$ sensors, as shown in Fig. 1. Assume there are $d$ sources present, where $d \leq M$. At the $n$th snapshot, the data model can be written as

$$\begin{aligned} \mathbf{x}(n) &= \mathrm{A}_x \mathbf{s}_x(n) + \boldsymbol{n}_x(n) \\ \mathbf{y}(n) &= \mathrm{A}_y \mathbf{s}_y(n) + \boldsymbol{n}_y(n). \end{aligned} \tag{1}$$

In this model, $\mathbf{x}(n) \in \mathbb{C}^M$ and $\mathbf{y}(n) \in \mathbb{C}^M$ are the output vectors of the two arrays, $\mathrm{A}_x$ and $\mathrm{A}_y$ are $\mathbb{C}^{M\times d}$ unambiguous directional matrices of the signals with respect to the geometry of the two arrays, both of which are full column rank, $\mathbf{n}_x(n) \in \mathbb{C}^M$ and $\mathbf{n}_y(n) \in \mathbb{C}^M$ are the zero-mean noise vectors of the two arrays, and $\mathbf{s}_x(t)$ and $\mathbf{s}_y(t)$ are the source signals arriving at the two arrays where $\mathbf{s}_x(t) = [s_{x1}(n), s_{x2}(n), \cdots, s_{xd}(n)]^T$ and $\mathbf{s}_y(t) = [s_{y1}(n), \mathbf{s}_{y2}(n), \cdots, s_{yd}(n)]^T$.

The composite data vector $\mathbf{z}(n) = [\mathbf{x}(n)^T \mathbf{y}(n)^T]^T$ has a covariance matrix

$$\mathrm{R}_{zz} = E[\mathbf{z}(n)\ \mathbf{z}(n)^T] = E\left[ \begin{pmatrix} \mathbf{x}(n) \\ \mathbf{y}(n) \end{pmatrix} \begin{pmatrix} \mathbf{x}(n)^T & \mathbf{y}(n)^T \end{pmatrix} \right] = \begin{bmatrix} \mathrm{R}_{xx} & \mathrm{R}_{xy} \\ \mathrm{R}_{yx} & \mathrm{R}_{yy} \end{bmatrix} \tag{2}$$

where $\mathrm{R}_{xx}$ and $\mathrm{R}_{yy}$ are the covariance matrices of $\mathbf{x}(n)$ and $\mathbf{y}(n)$, and $\mathrm{R}_{xy} = \mathrm{R}_{yx}^T$ is the cross-covariance matrix between $\mathbf{x}(n)$ and $\mathbf{y}(n)$. Defining the coherence matrix $\mathrm{C} = \mathrm{R}_{xx}^{-\frac{1}{2}} \mathrm{R}_{xy} \mathrm{R}_{yy}^{-\frac{H}{2}}$, and using the singular value decomposition (SVD), we obtain

$$\mathrm{C} = \mathrm{F}\Sigma\mathrm{G}^H \tag{3}$$

where F and G are the unitary matrices obtained from the SVD of C, and $H$ represents the Hermitian operator. $\Sigma$ is the canonical correlation matrix with

$$\Sigma = \begin{bmatrix} \Sigma_0 & \mathbf{0} \\ \mathbf{0} & \mathbf{0} \end{bmatrix}$$

where $\Sigma_0 \in \mathbb{R}^{d\times d}$ is a diagonal matrix, $d_0 (\leq d)$ is the rank of C, and $\lambda_1, \lambda_2, \cdots, \lambda_{d_0}$ are the first $d_0$ non-zero singular values of C.

For the following discussion, we define [4]

$$\mathrm{L}_1 = \mathrm{R}_{xx}^{-\frac{H}{2}} \mathrm{F},\ \mathrm{L}_2 = \mathrm{R}_{yy}^{-\frac{H}{2}} \mathrm{G},\ \mathrm{R}_1 = \mathrm{R}_{xx}^{\frac{1}{2}} \mathrm{F},\ \mathrm{R}_2 = \mathrm{R}_{yy}^{\frac{1}{2}} \mathrm{G} \tag{4}$$

with $\mathrm{L}_1^H \mathrm{R}_1 = \mathrm{L}_2^H \mathrm{R}_2 = I$. Let $\mathrm{F}_s$ be the first $d$ columns of F with respect to the first $d$ singular values of C including $d_0$ non-zero singular values, and $\mathrm{G}_s$ is similarly defined with respect to G. We then define

$$\mathrm{R}_{1s} = \mathrm{R}_{xx}^{\frac{1}{2}} \mathrm{F}_s\ , \quad \mathrm{R}_{2s} = \mathrm{R}_{yy}^{\frac{1}{2}} \mathrm{G}_s.$$

It follows that the composite covariance matrix $\mathrm{R}_{zz}$ can be written as,

$$\begin{aligned} \mathrm{R}_{zz} &= \begin{bmatrix} \mathrm{R}_{xx}^{\frac{1}{2}} \mathrm{F} & \mathbf{0} \\ \mathbf{0} & \mathrm{R}_{yy}^{\frac{1}{2}} \mathrm{G} \end{bmatrix} \begin{bmatrix} \mathrm{I} & \Sigma \\ \Sigma^H & \mathrm{I} \end{bmatrix} \begin{bmatrix} \mathrm{F}^H \mathrm{R}_{xx}^{\frac{H}{2}} & \mathbf{0} \\ \mathbf{0} & \mathrm{G}^H \mathrm{R}_{yy}^{\frac{H}{2}} \end{bmatrix} \\ &= \begin{bmatrix} \mathrm{R}_1 & \mathbf{0} \\ \mathbf{0} & \mathrm{R}_2 \end{bmatrix} \begin{bmatrix} \mathrm{I} & \Sigma \\ \Sigma^H & \mathrm{I} \end{bmatrix} \begin{bmatrix} \mathrm{R}_1^H & \mathbf{0} \\ \mathbf{0} & \mathrm{R}_2^H \end{bmatrix}. \end{aligned} \tag{5}$$

## III. Application of CCD

In this section, the covariance matrix of the source signals will be analyzed using the CCD framework. Then the relationship between the spatial correlation properties of the source signals and the canonical correlations of the observed signals will be derived. Additionally, it is demonstrated that the spatial correlations of the source signals can be captured perfectly by the canonical correlations of the observed signals if the SNR is sufficiently high.

Define the composite covariance matrix for the source signals $\mathbf{s}_x(t)$ and $\mathbf{s}_y(t)$ as

$$\mathrm{R}_{ss} = \begin{bmatrix} \mathrm{R}_{s_x s_x} & \mathrm{R}_{s_x s_y} \\ \mathrm{R}_{s_y s_x} & \mathrm{R}_{s_y s_y} \end{bmatrix}.$$

The spatial correlation coefficient $\rho_{ii}$ between the two random signals $s_{xi}(n)$ and $s_{yi}(n)$ with respect to the $i$th source signal $\mathbf{s}_i$ arriving at the x-array and y-array, respectively, can be written as

$$\rho_{ii} = \frac{E\{s_{xi}(n) s_{yi}^*(n)\}}{\sigma_{s_{xi}} \sigma_{s_{yi}}}, \quad i = 1, 2, \cdots, d,$$

where $\sigma_{s_{xi}}^2$ and $\sigma_{s_{yi}}^2$ are the variances of $s_{xi}(n)$ and $s_{yi}(n)$, respectively. If all the source signals are zero-mean and the different sources are uncorrelated with each other, then $\mathrm{R}_{ss}$ is composed of four diagonal sub-matrices, i.e.

$$\mathrm{R}_{ss} = \begin{bmatrix} \mathrm{R}_{s_x s_x} & \mathrm{R}_{s_x s_y} \\ \mathrm{R}_{s_y s_x} & \mathrm{R}_{s_y s_y} \end{bmatrix} = \begin{bmatrix} \Lambda_{s_{xx}} & \Lambda_{s_{xy}} \\ \Lambda_{s_{yx}} & \Lambda_{s_{yy}}, \end{bmatrix}, \tag{6}$$

where

$$\begin{aligned} \Lambda_{s_{xx}} &= \mathit{diag}[\sigma_{s_{x1}}^2, \sigma_{s_{x2}}^2, \cdots, \sigma_{s_{xd}}^2], \\ \Lambda_{s_{yy}} &= \mathit{diag}[\sigma_{s_{y1}}^2, \sigma_{s_{y2}}^2, \cdots, \sigma_{s_{yd}}^2], \\ \Lambda_{s_{xy}} &= \mathit{diag}[\rho_{11}\sigma_{s_{x1}}\sigma_{s_{y1}}, \rho_{22}\sigma_{s_{x2}}\sigma_{s_{y2}}, \cdots, \rho_{dd}\sigma_{s_{xd}}\sigma_{s_{yd}}], \\ \Lambda_{s_{yx}} &= \Lambda_{s_{xy}}^H. \end{aligned}$$

If the different sources are dependent on each other, then the composite source covariance matrix $\mathrm{R}_{ss}$ will not have the structure in (6). In this case, $\mathrm{R}_{ss}$ can be decomposed as

$$\mathrm{R}_{ss} = \begin{bmatrix} \tilde{\mathrm{R}}_1 & \mathbf{0} \\ \mathbf{0} & \tilde{\mathrm{R}}_2 \end{bmatrix} \begin{bmatrix} \mathrm{I} & \mathrm{P} \\ \mathrm{P}^H & \mathrm{I} \end{bmatrix} \begin{bmatrix} \tilde{\mathrm{R}}_1^H & \mathbf{0} \\ \mathbf{0} & \tilde{\mathrm{R}}_2^H \end{bmatrix} \tag{7}$$

where $\tilde{\mathrm{R}}_1$ and $\tilde{\mathrm{R}}_2$ are defined similar to $\mathrm{R}_1$ and $\mathrm{R}_2$ in (5), respectively, and P is the canonical correlation matrix of the sources. Here P is also called the spatial correlation matrix since it describes the spatial correlation properties of the arriving signals. Observing this CCD of $\mathrm{R}_{ss}$ for the special case of independent sources in (6), we have $\mathrm{P} = diag[\rho_{11}, \rho_{22}, \cdots, \rho_{dd}]$.

Combining the data model (1), the covariance matrix $\mathrm{R}_{zz}$ can be rewritten as

$$\mathrm{R}_{zz} = \begin{bmatrix} \mathrm{A}_x & \mathbf{0} \\ \mathbf{0} & \mathrm{A}_y \end{bmatrix} \begin{bmatrix} \tilde{\mathrm{R}}_1 & \mathbf{0} \\ \mathbf{0} & \tilde{\mathrm{R}}_2 \end{bmatrix} \begin{bmatrix} \mathrm{I} & \mathrm{P} \\ \mathrm{P}^H & \mathrm{I} \end{bmatrix} \begin{bmatrix} \tilde{\mathrm{R}}_1^H & \mathbf{0} \\ \mathbf{0} & \tilde{\mathrm{R}}_2^H \end{bmatrix} \times \begin{bmatrix} \mathrm{A}_x^H & \mathbf{0} \\ \mathbf{0} & \mathrm{A}_y^H \end{bmatrix} + \begin{bmatrix} \mathrm{R}_{n_x n_x} & \mathbf{0} \\ \mathbf{0} & \mathrm{R}_{n_y n_y} \end{bmatrix}. \tag{8}$$

Now, the middle term in (5) can also be written as,

$$\begin{bmatrix} \mathrm{I} & \Sigma \\ \Sigma^H & \mathrm{I} \end{bmatrix} = \begin{bmatrix} \mathrm{L}_1^H & \mathbf{0} \\ \mathbf{0} & \mathrm{L}_2^H \end{bmatrix} \mathrm{R}_{zz} \begin{bmatrix} \mathrm{L}_1 & \mathbf{0} \\ \mathbf{0} & \mathrm{L}_2 \end{bmatrix}. \tag{9}$$

Substituting (8) into (9) yields

$$\Sigma = \mathrm{L}_1^H \mathrm{A}_x \tilde{\mathrm{R}}_1 \mathrm{P} \tilde{\mathrm{R}}_2^H \mathrm{A}_y^H \mathrm{L}_2, \tag{10}$$

and

$$\mathrm{L}_1^H \mathrm{A}_x \tilde{\mathrm{R}}_1 \tilde{\mathrm{R}}_1^H \mathrm{A}_x^H \mathrm{L}_1 = \mathrm{I} - \mathrm{L}_1^H \mathrm{R}_{n_x n_x} \mathrm{L}_1, \tag{11a}$$

$$\mathrm{L}_2^H \mathrm{A}_y \tilde{\mathrm{R}}_2 \tilde{\mathrm{R}}_2^H \mathrm{A}_y^H \mathrm{L}_2 = \mathrm{I} - \mathrm{L}_2^H \mathrm{R}_{n_y n_y} \mathrm{L}_2. \tag{11b}$$

Define $\mathrm{M}_x = \mathrm{I} - \mathrm{L}_1^H \mathrm{R}_{n_x n_x} \mathrm{L}_1$, $\mathrm{M}_y = \mathrm{I} - \mathrm{L}_2^H \mathrm{R}_{n_y n_y} \mathrm{L}_2$. Alternatively, $\mathrm{M}_x$ can be expressed as

$$\mathrm{M}_x = \mathrm{F}^H (\mathrm{I} - \mathrm{R}_{xx}^{-\frac{1}{2}} \mathrm{R}_{n_x n_x} \mathrm{R}_{xx}^{-\frac{H}{2}}) \mathrm{F}. \tag{12}$$

If we perform an eigenvalue decomposition on the term $(\mathrm{I} - \mathrm{R}_{xx}^{-\frac{1}{2}} \mathrm{R}_{n_x n_x} \mathrm{R}_{xx}^{-\frac{H}{2}})$ in (12), $\mathrm{M}_x$ can be written as

$$\mathrm{M}_x = \mathrm{F}^H \mathrm{E}_x \Gamma_x \mathrm{E}_x^H \mathrm{F},$$

where $\Gamma_x$ is the eigenvalue matrix of $(\mathrm{I} - \mathrm{R}_{xx}^{-\frac{1}{2}} \mathrm{R}_{n_x n_x} \mathrm{R}_{xx}^{-\frac{H}{2}})$ and $\mathrm{E}_x$ is its unitary eigenvector matrix. It can be seen from (11a) that, since $\mathrm{L}_1^H$ and $\tilde{\mathrm{R}}_1$ are both full-rank and $\mathrm{A}_x$ has full-column rank, $rank\{\mathrm{M}_x\} = d$. Since F is full-rank, the matrix $(\mathrm{I} - \mathrm{R}_{xx}^{-\frac{1}{2}} \mathrm{R}_{n_x n_x} \mathrm{R}_{xx}^{-\frac{H}{2}})$ has $d$ non-zero eigenvalues, i.e. $\Gamma_x = diag[\gamma_{x1}, \gamma_{x2}, ..., \gamma_{xd}, 0, 0, ..0]$.

Define $\Gamma_{xs} = diag[\gamma_{x1}, \gamma_{x2}, ..., \gamma_{xd}]$ as the diagonal matrix containing the $d$ non-zero eigenvalues of $\Gamma_x$, and $\mathrm{E}_{xs}$ as the matrix consisting of the first $d$ eigenvectors corresponding to these eigenvalues. The matrix $\mathrm{M}_x$ can then be rewritten as

$$\mathrm{M}_x = \mathrm{F}^H \mathrm{E}_{xs} \Gamma_{xs} \mathrm{E}_{xs}^H \mathrm{F}. \tag{13}$$

According to (11a) and (13), the matrix $\tilde{\mathrm{R}}_1^H \mathrm{A}_x^H \mathrm{L}_1$ has full row rank and it has a right inverse $[\tilde{\mathrm{R}}_1^H \mathrm{A}_x^H \mathrm{L}_1]^\dagger$ with full column rank, where $[\cdot]^\dagger$ denotes the right pseudo-inverse operation. It follows that

$$\mathrm{L}_1^H \mathrm{A}_x \tilde{\mathrm{R}}_1 = \mathrm{F}^H \mathrm{E}_{xs} \Gamma_{xs} \mathrm{E}_{xs}^H \mathrm{F} [\tilde{\mathrm{R}}_1^H \mathrm{A}_x^H \mathrm{L}_1]^\dagger.$$

Therefore, the columns of the matrix $\mathrm{L}_1^H \mathrm{A}_x \tilde{\mathrm{R}}_1$ span the same subspace as that spanned by the columns of $\mathrm{F}^H \mathrm{E}_{xs} \Gamma_{xs}^{\frac{1}{2}}$, where $\Gamma_{xs}^{\frac{1}{2}} = diag[\gamma_{x1}^{\frac{1}{2}}, \gamma_{x2}^{\frac{1}{2}}, ..., \gamma_{xd}^{\frac{1}{2}}]$. There exists an unique $d \times d$ non-singular matrix $\mathrm{U}_x$ satisfying

$$\mathrm{L}_1^H \mathrm{A}_x \tilde{\mathrm{R}}_1 = \mathrm{F}^H \mathrm{E}_{xs} \Gamma_{xs}^{\frac{1}{2}} \mathrm{U}_x. \tag{14}$$

From (11a), we also have

$$\mathrm{L}_1^H \mathrm{A}_x \tilde{\mathrm{R}}_1 (\mathrm{L}_1^H \mathrm{A}_x \tilde{\mathrm{R}}_1)^H = \mathrm{F}^H \mathrm{E}_{xs} \Gamma_{xs}^{\frac{1}{2}} (\mathrm{F}^H \mathrm{E}_{xs} \Gamma_{xs}^{\frac{1}{2}})^H.$$

Thus, the matrix $\mathrm{U}_x$ is also unitary. Similarly, we have

$$\mathrm{L}_2^H \mathrm{A}_y \tilde{\mathrm{R}}_2 = \mathrm{G}^H \mathrm{E}_{ys} \Gamma_{ys}^{\frac{1}{2}} \mathrm{U}_y, \tag{15}$$

where $\mathrm{U}_y$ is also an unitary matrix. Substituting (14) and (15) into (10), we get

$$\Sigma = \mathrm{F}^H \mathrm{E}_{xs} \Gamma_{xs}^{\frac{1}{2}} \mathrm{U}_x \mathrm{P} \mathrm{U}_y^H \Gamma_{ys}^{\frac{1}{2}} \mathrm{E}_{ys}^H \mathrm{G}, \tag{16}$$

which can also be written as

$$\Sigma = \mathrm{F}^H \mathrm{E}_x \begin{bmatrix} \Gamma_{xs}^{\frac{1}{2}} & \mathbf{0} \\ \mathbf{0} & \mathbf{0} \end{bmatrix} \begin{bmatrix} \mathrm{U}_x \mathrm{P} \mathrm{U}_y^H & \mathbf{0} \\ \mathbf{0} & \mathbf{0} \end{bmatrix} \begin{bmatrix} \Gamma_{ys}^{\frac{1}{2}} & \mathbf{0} \\ \mathbf{0} & \mathbf{0} \end{bmatrix} \mathrm{E}_y^H \mathrm{G}.$$

Let $\mathrm{F}_1 = \mathrm{E}_x^H \mathrm{F}$, and $\mathrm{G}_1 = \mathrm{E}_y^H \mathrm{G}$. Since $\mathrm{E}_x, \mathrm{E}_y, \mathrm{F}$ and G are unitary matrices, it follows that $\mathrm{F}_1$ and $\mathrm{G}_1$ are both unitary and we have

$$\mathrm{F}_1 \begin{bmatrix} \Sigma_0 & \mathbf{0} \\ \mathbf{0} & \mathbf{0} \end{bmatrix} \mathrm{G}_1^H = \begin{bmatrix} \Gamma_{xs}^{\frac{1}{2}} \mathrm{U}_x \mathrm{P} \mathrm{U}_y^H \Gamma_{ys}^{\frac{1}{2}} & \mathbf{0} \\ \mathbf{0} & \mathbf{0} \end{bmatrix}, \tag{17}$$

where the left side is the SVD of the right side. This shows that the diagonal elements of $\Sigma_0$ are the singular values of the matrix $\Gamma_{xs}^{\frac{1}{2}} \mathrm{U}_x \mathrm{P} \mathrm{U}_y^H \Gamma_{ys}^{\frac{1}{2}}$, where P represents the spatial correlation matrix of the sources, and $\Gamma_{xs}^{\frac{1}{2}}$ and $\Gamma_{ys}^{\frac{1}{2}}$ represent the noise-to-signal ratio information in the two arrays. Unitary matrices $\mathrm{U}_x$ and $\mathrm{U}_y$ are related to the matrices $\mathrm{A}_x$ and $\mathrm{A}_y$ by (14) and (15), which contain the geometry information between the sonar arrays and sources. Therefore, the canonical correlations of the observed data can be used to analyze the spatial correlation of the sources. However, this is dependent on the noise-to-signal ratio and array geometry. Since the rank of $\Gamma_{xs}^{\frac{1}{2}} \mathrm{U}_x \mathrm{P} \mathrm{U}_y^H \Gamma_{ys}^{\frac{1}{2}}$ is equal to $rank\{\mathrm{P}\}$, the number of non-zero diagonal elements of P is equal to $d_0$, i.e. the number of non-zero diagonal elements of $\Sigma_0$. Therefore, for independent sources, the number of non-zero diagonal elements of $\Sigma_0$ can be used to estimate the number of sources.

If the SNR is sufficiently high, the effects of noise can be ignored in comparison to the signal. However, in this case the covariance matrices $\mathrm{R}_{xx}$ and $\mathrm{R}_{yy}$ both have rank $d$, i.e. they are not full-rank. Using this assumption, the CCD of $\mathrm{R}_{zz}$ in (5) can be rewritten as

$$\mathrm{R}_{zz} = \begin{bmatrix} \mathrm{R}_1 & \mathbf{0} \\ \mathbf{0} & \mathrm{R}_2 \end{bmatrix} \begin{bmatrix} \mathrm{I}_u & \Sigma \\ \Sigma^H & \mathrm{I}_v \end{bmatrix} \begin{bmatrix} \mathrm{R}_1^H & \mathbf{0} \\ \mathbf{0} & \mathrm{R}_2^H \end{bmatrix}, \tag{18}$$

where

$$\mathrm{I}_u = \begin{bmatrix} \mathrm{I}_{d \times d} & \mathbf{0} \\ \mathbf{0} & \mathbf{0} \end{bmatrix}, \ \mathrm{I}_v = \begin{bmatrix} \mathrm{I}_{d \times d} & \mathbf{0} \\ \mathbf{0} & \mathbf{0} \end{bmatrix}.$$

In this case, (11a) and (11b) become

$$\mathrm{L}_1^H \mathrm{A}_x \tilde{\mathrm{R}}_1 \tilde{\mathrm{R}}_1^H \mathrm{A}_x^H \mathrm{L}_1 = \mathrm{I}_u,$$
$$\mathrm{L}_2^H \mathrm{A}_y \tilde{\mathrm{R}}_2 \tilde{\mathrm{R}}_2^H \mathrm{A}_y^H \mathrm{L}_2 = \mathrm{I}_v.$$

It follows that

$$\mathrm{A}_x\tilde{\mathrm{R}}_1\tilde{\mathrm{R}}_1^H\mathrm{A}_x^H = \mathrm{R}_1\mathrm{I}_u\mathrm{R}_1^H = \mathrm{R}_{1s}\mathrm{R}_{1s}^H,$$
$$\mathrm{A}_y\tilde{\mathrm{R}}_2\tilde{\mathrm{R}}_2^H\mathrm{A}_y^H = \mathrm{R}_2\mathrm{I}_v\mathrm{R}_2^H = \mathrm{R}_{2s}\mathrm{R}_{2s}^H.$$

From the above, we note that there exists two unique unitary matrices, $\mathrm{U}_x$ and $\mathrm{U}_y$, satisfying

$$\mathrm{A}_x\tilde{\mathrm{R}}_1 = \mathrm{R}_{1s}\mathrm{U}_x, \quad \mathrm{A}_y\tilde{\mathrm{R}}_2 = \mathrm{R}_{2s}\mathrm{U}_y. \tag{19}$$

Substituting (19) into (10), we obtain

$$\Sigma = \mathrm{L}_1^H\mathrm{R}_{1s}\mathrm{U}_x\mathrm{P}\mathrm{U}_y^H\mathrm{R}_{2s}^H\mathrm{L}_2.$$

Using $\mathrm{L}_{1s}^H\mathrm{R}_{1s} = \mathrm{R}_{2s}^H\mathrm{L}_{2s} = I$ in (4), we get

$$\Sigma_0 = \mathrm{U}_x\mathrm{P}\mathrm{U}_y^H.$$

Since $\Sigma_0$ and P are diagonal, it follows that

$$\Sigma_0 = \mathrm{P}. \tag{20}$$

This result shows that, if the SNR is sufficiently high, the canonical correlations of the observed data will be equal to those of the sources. This result demonstrates that canonical correlations are invariant to the linear transformation of the two-channel data if the transformation matrices $\mathrm{A}_x$ and $\mathrm{A}_y$ are full-column rank. Furthermore, if the sources are zero-mean and independent, their spatial correlation coefficients will be equal to the canonical correlations.

## IV. Circulant Covariance Matrices

This section analyzes the relationship between the canonical correlations of the observed data and those of the sources when the correlations between spatially stationary signals at different sensors in the array are only dependent on the sensor element spacing. In this case, the covariance matrices $\mathrm{R}_{xx}, \mathrm{R}_{n_xn_x}$ become circulant, and can be written as [7]

$$\mathrm{R}_{xx} = \begin{bmatrix} r_x(0) & r_x(M-1) & \cdots & r_x(1) \\ r_x(1) & r_x(0) & \cdots & r_x(2) \\ \cdots & \cdots & \cdots & \cdots \\ r_x(M-1) & r_x(M-2) & \cdots & r_x(0) \end{bmatrix}$$

$$\mathrm{R}_{n_xn_x} = \begin{bmatrix} r_{n_x}(0) & r_{n_x}(M-1) & \cdots & r_{n_x}(1) \\ r_{n_x}(1) & r_{n_x}(0) & \cdots & r_{n_x}(2) \\ \cdots & \cdots & \cdots & \cdots \\ r_{n_x}(M-1) & r_{n_x}(M-2) & \cdots & r_{n_x}(0) \end{bmatrix}.$$

Therefore, both $\mathrm{R}_{xx}$ and $\mathrm{R}_{n_xn_x}$ have orthogonal representations

$$\mathrm{R}_{xx} = \mathrm{W}_M\Omega_x\mathrm{W}_M^H,$$
$$\mathrm{R}_{n_xn_x} = \mathrm{W}_M\Omega_{n_x}\mathrm{W}_M^H,$$

where $[\mathrm{W}_M]_{m,n} = e^{j2\pi mn/M}$ is the $M \times M$ DFT matrix, $m, n \in [0, M-1]$. The diagonal elements of the matrices $\Omega_x$ and $\Omega_{n_x}$ contain the DFT coefficients of the first column of $\mathrm{R}_{xx}$ and $\mathrm{R}_{n_xn_x}$, respectively, i.e.,

$$\Omega_x = diag[\omega_x(0), \omega_x(1), \cdots, \omega_x(M-1)],$$
$$\Omega_{n_x} = diag[\omega_{n_x}(0), \omega_{n_x}(1), \cdots, \omega_{n_x}(M-1)],$$

where

$$\omega_x(l) = \sum_{m=0}^{M-1} r_x(m)e^{-j2\pi ml/M}, \ \ l \in [0, M-1]$$
$$\omega_{n_x}(l) = \sum_{m=0}^{M-1} r_{n_x}(m)e^{-j2\pi ml/M}, \ \ l \in [0, M-1].$$

Here, $\omega_x(l)$ and $\omega_{n_x}(l)$ are the power spectra of $x(t)$ and $n_x(t)$, respectively at frequencies $l \in [0, M-1]$. Define $\mathrm{Q}_x = \mathrm{R}_{xx}^{-\frac{1}{2}}\mathrm{R}_{n_xn_x}\mathrm{R}_{xx}^{-\frac{H}{2}}$, then

$$\mathrm{Q}_x = \mathrm{W}_M\Omega_x^{-\frac{1}{2}}\Omega_{n_x}\Omega_x^{-\frac{1}{2}}\mathrm{W}_M^H, \tag{21}$$

and

$$\mathrm{M}_x = \mathrm{F}^H(\mathrm{I} - \mathrm{Q}_x)\mathrm{F}. \tag{22}$$

The eigenvalues of $(\mathrm{I} - \mathrm{Q}_x)$ can thus be written as

$$\gamma_{xl} = 1 - \frac{\omega_{n_x}(l-1)}{\omega_x(l-1)}, \quad l \in [1, d]$$

with $\gamma_{xl} = 0, \ \ l > d$.

If $n_x(t)$ is white, i.e. $\omega_{n_x}(l) = \sigma_{nx}^2 = p_{nx}$, and the power spectrum of $\mathbf{x}(t)$ can be approximated by

$$\omega_x(l) = \begin{cases} p_x & , \ \ l \in [0, d-1] \\ p_{nx} & , \ \ l \in [d, M-1] \end{cases}$$

then it follows that

$$\Gamma_{xs}^{\frac{1}{2}} = \sqrt{1 - \frac{p_{n_x}}{p_x}}\ \mathrm{I}_{d\times d}, \tag{23}$$

and similarly,

$$\Gamma_{ys}^{\frac{1}{2}} = \sqrt{1 - \frac{p_{n_y}}{p_y}}\ \mathrm{I}_{d\times d}. \tag{24}$$

From (17),(23), and (24), the relationship between $\Sigma_0$ and P becomes

$$\Sigma_0 = \sqrt{(1 - \frac{p_{n_x}}{p_x})(1 - \frac{p_{n_y}}{p_y})}\ \mathrm{P}. \tag{25}$$

This special case demonstrates how the noise level affects the spatial correlation analysis of the source signals using CCD. The effective factor in (25) is proportional to the square roots of the eigenvalues of the matrices $(\mathrm{I} - \mathrm{Q}_x)$ and $(\mathrm{I} - \mathrm{Q}_y)$, which in this special case are related to the SNR of the signals received by both arrays.

## V. Simulations and Discussions

In this section, simulation results are presented in order to show the relationship between the canonical correlations of the observed signals and the source spatial correlation characteristic for two uniform linear arrays for a near-field source case. Specifically, we analyze how different levels of noise impact the canonical correlations. In addition, we analyze the impacts of changes in the geometry between the sources and the array, since this affects the directional matrices $\mathrm{A}_x$ and $\mathrm{A}_y$ in the near-field case.

Fig. 2 shows the position of the sources with respect to the two arrays with $M$ elements each. The inter-element spacing is $\lambda/4$ and the displacement of the two arrays is $D = 10\lambda$, where

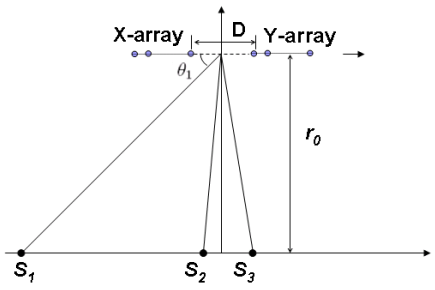


Fig. 2. Positions of the sources and two arrays.

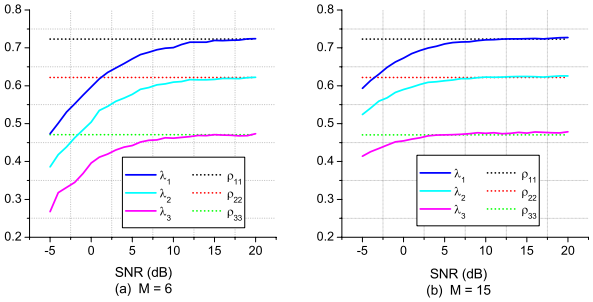


Fig. 3. Impact of SNR on the canonical correlations.

$\lambda = 0.1m$. There are $d = 3$ sources that are located at different points along a line as shown in Fig. 2. The angles between the sources and the center of the two arrays are $\theta_1 = 34.3^o$, $\theta_2 = 85.9^o$, and $\theta_3 = 105.5^o$. The elevation of the sonar arrays (platform) from the plane of the sources is kept constant at $r_0 = 3m$. The following assumptions are made:

1) The sources are zero-mean and independent random signals. For this simulation, they are modeled by a first-order auto-regressive (AR) model with coefficients $\phi_i$, i.e. at the $n$th snapshot,

$$s_i(n) = \phi_i s_i(n-1) + \varepsilon_i(n), \quad i \in [1, d] \tag{26}$$

where $\varepsilon_i(n)'s$ are the driving processes that are assumed to be independent zero-mean white Gaussian. In this case, the variance of each source is $\sigma^2_{s_i} = \frac{\sigma^2_{\varepsilon_i}}{1-\phi_i^2}$.

2) The arriving random signals at the two arrays emanated from the same source satisfy coherence models given by

$$\begin{aligned} s_{xi}(n) &= \eta_{xi} s_i(n) + \xi_{xi}(n), \\ s_{yi}(n) &= \eta_{yi} s_i(n) + \xi_{yi}(n), \quad \forall n, i \in [1, d] \end{aligned} \tag{27}$$

where $\xi_{xi}(n)'s$ and $\xi_{yi}(n)'s$ are independent zero-mean additive white Gaussian noise processes, and $\eta_{xi}$ and $\eta_{yi}$ represent the fading and phasing effects on the signals. These effects are modeled as $\eta_{xi} = e^{-\alpha r_{xi} + j\beta_{xi}}$ and $\eta_{yi} = e^{-\alpha r_{yi} + j\beta_{yi}}$, where $\alpha = 0.025$ is the absorption coefficient, $r_{xi}$ and $r_{yi}$ are the ranges of the $i$th source with respect to the center of each array, and $\beta_{xi}$ and $\beta_{yi}$ are uniformly distributed random variables over $[-\Delta, \Delta]$ representing the phasing effects. Then, the spatial correlation coefficients are

$$\rho_{ii} = \frac{\frac{sin^2\Delta}{\Delta^2}}{\sqrt{(1 + \frac{\sigma^2_{\xi_{xi}}}{\sigma^2_{\eta_{xi}}\sigma^2_{s_i}})(1 + \frac{\sigma^2_{\xi_{yi}}}{\sigma^2_{\eta_{yi}}\sigma^2_{s_i}})}}, \; i = 1, 2, \cdots, d, \tag{28}$$

and $\rho_{ij} = 0, \; i \neq j$.

Using the above assumptions, the covariance matrix of the sources will have the form given in (6). The parameters of the AR models were selected as follows. The coefficients of the AR model in (26) for the three sources were chosen to be $\phi_1 = 0.6371$, $\phi_2 = 0.2881$, and $\phi_3 = 0.3128$, and the sources have identical variances $\sigma^2_{\mathbf{s}_1} = \sigma^2_{\mathbf{s}_2} = \sigma^2_{\mathbf{s}_3} = 1$. The parameters of the coherence model were selected as $\sigma^2_{\xi_{x1}} = \sigma^2_{\xi_{y1}} = 0.2$, $\sigma^2_{\xi_{x2}} = \sigma^2_{\xi_{y2}} = 0.4$ , and $\sigma^2_{\xi_{x3}} = \sigma^2_{\xi_{y3}} = 0.8$ . The coherent loss effects $\eta_{xi}$ and $\eta_{yi}$, $i = 1, 2, 3$, can be calculated from the given geometry parameters of the sources and arrays, and a random draw of $\beta_{xi}$ and $\beta_{yi}$ with $\Delta = \frac{\pi}{6}$.

According to (28), the spatial correlation coefficients of these sources between the two arrays were found to be $\rho_{11} = 0.7231$, $\rho_{22} = 0.6217$ and $\rho_{33} = 0.4705$ for the locations of sources and arrays as shown in Fig. 2. The relationship between the canonical correlations and the spatial correlation coefficients are validated for different SNRs in Fig. 3. These results were calculated using 50 Monte-Carlo simulations. When the SNR is sufficiently high (i.e. $> 15dB$), the canonical correlations are very close to the spatial correlation coefficients (horizontal lines), hence proving the result in (20). Additionally, Figs. 3(a) and (b) show that as the number of sensor elements increases, the impact of the noise on the canonical correlations reduces significantly even for lower values of SNR. CCD transforms the observed data into its canonical coordinates where the noise is also projected onto the same basis. For the $M = 15$ case, the source signals are still projected onto the first three canonical coordinates while the noise is projected onto all of the 15 coordinates as opposed to only 6, hence reducing the overall impact of noise.

The range between the sources and the arrays will affect the spatial correlation coefficients according to the model in (27). To study this effect we consider a case where the sources and the x-array are kept stationary, while the y-array is moved on the same line of the two arrays such that the displacement of the two arrays and the ranges of the sources to the y-array are changed. Figs. 4(a) and (b) illustrate these results, where the dotted curves show the effect of increasing $D$ on the spatial correlation coefficients of the sources $\rho_{11}, \rho_{22}, \rho_{33}$ calculated using (28), while the solid curves are the plots of the canonical correlations obtained using (5). Fig. 4(a) shows the case when $SNR = 20dB$ and $M = 6$ and Fig. 4(b) shows the case when $SNR = 20dB$ and $M = 15$. As can be seen the spatial correlation coefficients will become smaller for the larger array separation due to the increased coherence loss. We also notice that there is no significant difference between the dotted curves in these two figures. When the number of elements is increased to $M = 15$, the change in the size of array affects the

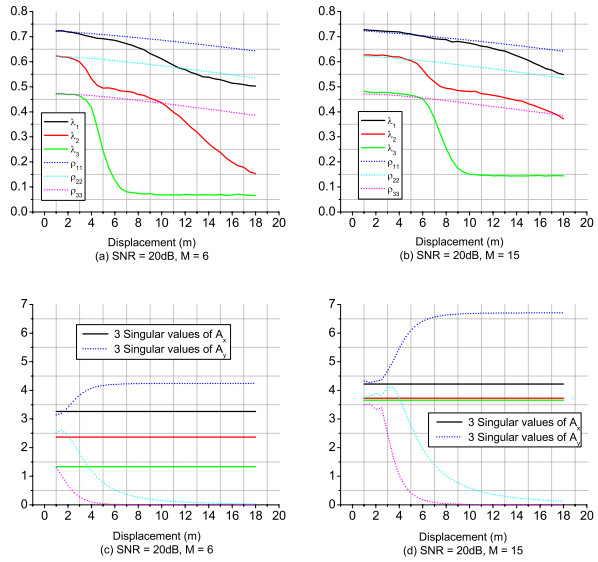


Fig. 4. Impact of displacement of the two arrays on the canonical correlations.

ranges of the sources to the center of each array, but this change in ranges is still not large enough to impact $\sigma^2_{\eta_{xi}}$ and $\sigma^2_{\eta_{yi}}$ in (28) significantly due to the inter-element spacing being only $\lambda/4$. Fig. 4(a) shows that canonical correlations can closely measure the spatial correlation coefficients of the sources under sufficiently high SNR when $D \leq 3m$. However, as $D$ increases, the solid curves differ from the dotted curves very rapidly. As mentioned before, the locations of the sources with respect to the arrays impact the structures of the matrices $\mathrm{A}_x$ and $\mathrm{A}_y$, which are required to be full-column rank in the derivations in Section III. For large displacement $D$, i.e. when the y-array is moved farther, the rank of $\mathrm{A}_y$ is reduced due to the change in the geometry of the sources with respect to the y-array. Figs. 4(c) and (d) show the singular values of the matrices $\mathrm{A}_x$ and $\mathrm{A}_y$ under different displacements $D$ for the cases in Figs. 4(a) and (b). From Fig. 4(c), we can see that the singular values of $\mathrm{A}_x$ are kept constant, and those of $\mathrm{A}_y$ change significantly as $D$ increases. Especially, for $D > 3m$, one singular value of $\mathrm{A}_y$ falls to zero very rapidly, which correlates well with the result in Figs. 4(a). Therefore, the canonical correlations will be affected by the locations of the sources and the arrays. For the arrays with $M = 15$, we observe from Figs. 4(b) and (d) that the impact of geometry on canonical correlations is substantially reduced. This is particularly evident in Fig. 4(d), which shows that, as opposed to the results in Fig. 4(c), one of the singular values becomes close to zero only when $D > 5.5m$. Thus, the arrays with more elements remain more robust to coherence loss in sparse sonar arrays.

## VI. Conclusions

In this paper we showed that the canonical correlations of the signals observed by two sensor arrays can be used to analyze the spatial correlation properties of the sources assuming that the array directional matrices $\mathrm{A}_x$ and $\mathrm{A}_y$ are both full column rank. CCD was then used to transform the observed data of the two arrays into its canonical coordinates. It was observed that the canonical correlations are nearly equal to the spatial correlation coefficients of the independent sources when the SNR is sufficiently high. The noise and array geometry can also affect the canonical correlations. It was shown through simulations that the canonical correlations differ from the spatial correlation coefficients as the SNR decreases or the array displacement increases. Simulations also showed that these impacts can be partially reduced if more array elements are used. With more elements, the canonical correlations can more accurately measure the spatial correlation coefficients under lower SNR or larger array displacement compared to the case of less elements.

## Acknowledgment

This research was supported by the Office of Naval Research (ONR 32MCM) under contract #N00014-07-1-0542.

## References

[1] H. Hotelling, "Relations between two sets of variates," *Biometrika*, vol.28, pp.321-377, 1936.

[2] K. M. Wong, Q. Wu, and P. Stoica,"Generalized correlation decomposition applied to array processing in unknown noise environments," in *Advances in spectrum analysis and array processing Vol. III*, S. Haykin, Ed., pp. 219, Prentice-Hall, Upper Saddle River, NJ, USA, 1995.

[3] W.G. Chen, J.P. Reilly, K.M. Wong, "Detection of the number of signals in noise with unknown, non-white covariance matrices," *Proc. of ICASSP*, vol.5, pp.377 - 380, Mar 1992.

[4] Qiang Wu and Kon Max Wong, "UN-MUSIC and UN-CLE: An Application of Generalized Correlation Analysis to the Estimation of the Direction of Arrival of Signals in Unknown Correlated Noise," *IEEE Trans. on Signal Processing*, vol.42, pp.2331-2343, Sep. 1994.

[5] Qiang Wu and Kon Max Wong, "Estimation of DOA in Unknown Noise: Performance Analysis of UN-MUSIC and UN-CLE, and the Optimality of CCD," *IEEE Trans. on Signal Processing*, vol.43, pp.454-468, Sep. 1995.

[6] Gaoming Huang, Luxi yang and Zhenya He, "Time-Delay Direction Finding Based on Canonical Correlation Analysis," *Proc. of ISCAS*, pp.5409-5412, May 2005.

[7] Louis L. Scharf and Clifford T. Mullis, "Canonical Coordinates and the Geometry of Inference, Rate, and Capacity," *IEEE Trans. on Signal Processing*, vol.48, pp.824-831, Mar 2000.

[8] Ali Pezeshki, Louis L. Scharf, Mahmood R. Azimi-Sadjadi and Yingbo Hua, "Two-Channel Constrained Least Squares Problems: Solutions Using Power Methods and Connections with Canonical Coordinates," *IEEE Trans. on Signal Processing*, vol.53, pp.121-135, Jan 2005.

[9] Mahmood R. Azimi-Sadjadi, Ali Pezeshki, Robert L. Wade, "Coherence analysis using canonical coordinate decomposition with applications to sparse processing and optimal array deployment," *Proc. of SPIE*, Vol.5417, pp.43-50, 2004.